Residues 48 and 82 at the N-Terminal Hydrophobic Pocket of Rabbit Skeletal Muscle Troponin-C Photo-Cross-Link to Met121 of Troponin-I[†]

Yin Luo,[‡] John Leszyk,[§] Yude Qian,[‡] John Gergely,[‡,||,⊥] and Terence Tao*[,‡,#,▽]

Muscle Research Group, Boston Biomedical Research Institute, Boston, Massachusetts 02114, Neurology Service, Massachusetts General Hospital, Boston, Massachusetts 02114, Department of Biological Chemistry and Molecular Pharmacology and Department of Neurology, Harvard Medical School, Boston, Massachusetts 02115, Department of Biochemistry, Tufts University School of Medicine, Boston, Massachusetts 02111, and Worcester Foundation Microsequencing Lab and Department of Biochemistry, University of Massachusetts School of Medicine, Shrewsbury, Massachusetts 01545

Received October 13, 1998; Revised Manuscript Received March 22, 1999

ABSTRACT: It has been proposed [Herzberg et al. (1986) *J. Biol. Chem. 261*, 2638−2644], and confirmed by structural studies [Gagne et al. (1995) *Nat. Struct. Biol. 2*, 784−789], that the binding of Ca^{2+} to the triggering sites in troponin-C (TnC) causes the opening of the N-terminal hydrophobic pocket bound by the B, C, and D helices. This conformational change is believed to provide an additional binding site for troponin-I (TnI) and to lead to further events in the Ca^{2+} regulation process. To answer the question of which part of TnI interacts with this hydrophobic patch of TnC, we constructed two TnC mutants, each with a single cysteine, one at residue 48 between helices B and C and the other at residue 82 on the D helix. Each mutant was labeled with the photoactivatable cross-linker benzophenone-4-iodoacetamide, followed by reconstitution and UV irradiation. Studies were made in the binary complex composed of TnC and TnI, the ternary complex composed of TnC, TnI, and troponin-T (TnT), and the synthetic thin filament composed of troponin, tropomyosin, and F-actin. TnC−TnI photo-cross-linking was observed for both mutants and for all three types of complexes. Although no Ca^{2+} dependence in the photo-cross-linking was observed on the binary and ternary complexes, the extent of cross-linking was reduced in the absence vs the presence of Ca^{2+} in the thin filament. TnI Met121, five residues from the C-terminus of the inhibitory region, was identified as the cross-linking site for both TnC mutants using microsequencing and mass spectrometry following proteolysis. These results, obtained with intact TnC·TnI complexes, indicate that the TnI segment containing Met121 is in close contact with the N-terminal hydrophobic patch of TnC, and that in the thin filament the segment containing this residue moves away slightly from the hydrophobic patch in the absence of Ca^{2+}, possibly triggering the translocation of the actin-binding region(s) of TnI toward actin.

The molecular basis for force generation in muscle is a cyclic interaction between myosin heads on the thick filaments and actin in the thin filaments, resulting in the sliding of the two filaments with respect to each other. In striated muscle this process is initiated by the binding of Ca^{2+} to troponin C (TnC),[1] the Ca^{2+}-binding subunit of the troponin (Tn) complex in the thin filaments. This results in a series of conformational changes in TnC as well as in TnI and TnT, the inhibitory and tropomyosin-anchoring subunits, respectively, of Tn, transmitting the triggering Ca^{2+} signal to tropomyosin (Tm) and actin (for reviews, see refs *1*−*4*).

The structure of TnC on the atomic level has been well characterized (*5*−*7*). It consists of two globular domains connected by an α-helix. The C-terminal domain contains the two high-affinity Ca^{2+}-binding sites that also bind Mg^{2+} at lower affinity; the N-terminal domain contains the two low-affinity Ca^{2+}-specific sites that have been shown to be the physiologically relevant activation sites (*8*, *9*). It was

[†] This work was supported by National Institutes of Health Grants AR21673 (to T.T.) and HL5949 (to J.G.).

* To whom correspondence should be addressed at the Boston Biomedical Research Institute, 20 Staniford St., Boston, MA 02114. Telephone: 617-912-0370. Fax: 617-912-0308. E-mail: tao@bbri.harvard.edu.

[‡] Boston Biomedical Research Institute.

[§] University of Massachusetts School of Medicine.

[||] Massachusetts General Hospital.

[⊥] Department of Biological Chemistry and Molecular Pharmacology, Harvard Medical School.

[#] Department of Neurology, Harvard Medical School.

[▽] Tufts University School of Medicine.

[1] Abbreviations: Tn, troponin; TnC, troponin-C; TnI, troponin-I; TnT, troponin-T; Tm, tropomyosin; TnC48, recombinant TnC with a single cysteine at residue 48; TnC82, recombinant TnC with a single cysteine at residue 82; BP-IA, benzophenone-4-iodoacetamide; BP-TnC48 and BP-TnC82, TnC48 and TnC82 with benzophenone attached to their cysteines; CP-Mal, 7-diethylamino-3-(4′-maleimidylphenyl)-4-methylcoumarin; CP-TnI, CP-Mal-labeled recombinant TnI with a single cysteine at residue 133; BP-C48-I and BP-C82-I, photo-cross-linking product of BP-TnC48 or BP-TnC82 with TnI; BP-C48-T and BP-C82-T, photo-cross-linking product of BP-TnC48 or BP-TnC82 with TnT; DTT, dithiothreitol; EDTA, ethylenediaminetetraacetic acid; EGTA, ethylene glycol bis(β-aminoethyl ether)-*N*,*N*,*N*′,*N*′-tetraacetic acid; CNBr, cyanogen bromide; HEPES, *N*-(2-hydroxyethyl)piperazine-*N*′-2-ethanesulfonic acid; Tris, tris(hydroxymethyl)aminomethane; GmdHCl, guanidinium chloride; Hse, homoserine; HPLC, high-performance liquid chromatography; MALDI-TOF, matrix-assisted laser desorption/ionization time-of-flight mass spectrometry; SDS−PAGE, sodium dodecyl sulfate−polyacrylamide gel electrophoresis.

10.1021/bi9824341 CCC: $18.00
Published on Web 04/24/1999

noticed (*6*) over a decade ago that although the two domains are highly similar in amino acid sequence and overall tertiary folding, the two differ in one important aspect: in the Ca^{2+}-bound C-terminal domain, helices E, F, and G form a hydrophobic surface that is relatively solvent-exposed; in contrast, in the Ca^{2+}-free N-terminal domain, the pocket formed by the equivalent helices B, C, and D is closed and relatively inaccessible to the solvent. It was proposed by these authors that, upon the binding of Ca^{2+} to the activation sites, the N-terminal hydrophobic pocket opens via the movement of the B and C helices away from the D helix, providing an additional interaction site for some segment of TnI (*10*). The occurrence of this Ca^{2+}-induced conformational change in the N-terminal domain of TnC was later confirmed by fluorescence (*11*), NMR (*12*), and X-ray crystallographic (*13, 14*) studies. That this opening is functionally important was demonstrated earlier by mutagenesis studies, which showed that by inhibiting or preventing the opening, activation was impaired (*15*) or lost (*16*).

In contrast to the wealth of information on TnC, much less is known about TnI. Some notable features include the following: (1) TnI has an inhibitory region roughly in the middle of the molecule which is capable of binding to Tm·actin filaments and inhibiting actomyosin activity, as well as interacting with TnC in a Ca^{2+}-dependent manner (*17*). (2) In a low-resolution model based on low-angle X-ray and neutron scattering studies (*18*), TnI is pictured as an elongated strand that coils over and between the two domains of TnC. (3) TnI interacts with TnC in an antiparallel manner; i.e., its N-terminal region interacts with the C-terminal domain of TnC and vice versa (*19, 20*). (4) A peptide containing residues 128−148 also binds to Tm·actin filaments and weakly inhibits actomyosin ATPase activity by itself (*21*). (5) The region corresponding to residues 116−131 (adjacent to the inhibitory region) weakens the inhibition of Tm−acto-S1 ATPase activity by the inhibitory region if the peptide is not extended to residue 148. But it enhances the binding of the inhibitory region to TnC in a Ca^{2+}-dependent manner and is critical for the Ca^{2+}-TnC-induced release of the inhibition of the activity (*21*). (6) NMR studies on the N-terminal half of chicken skeletal TnC reveal that the largest changes in chemical shifts induced by the addition of TnI peptide 115−131 are for residues located in the N-terminal hydrophobic pocket of TnC, indicating that this peptide is able to interact with the hydrophobic pocket (*22*).

From the foregoing it seems clear that the primary conformational transition in TnC in response to Ca^{2+} activation is the opening of its N-terminal hydrophobic pocket. The key question that remains is how this conformational transition in TnC is transmitted to TnI, and what changes occur in TnI that lead to further events in the regulatory process.

In this work we set out to identify, in the intact TnC·TnI complexes, the TnI residue or segment interacting with the N-terminal hydrophobic pocket of TnC using photo-cross-linkers placed on Cys residues introduced into TnC by site-directed mutagenesis. We constructed two mutant TnC's, each with a single cysteine at position 48 or 82. After attachment of the bifunctional photoactivatable cross-linker benzophenone-4-iodoacetamide (BP-IA) at these engineered cysteines, the labeled TnC's were reconstituted with TnI and other thin filament proteins, followed by UV irradiation to elicit photo-cross-linking. The site of cross-linking in TnI could be identified by microsequencing and mass spectrometric analysis of the cross-linking product.

Compared with other methods, this approach has the advantage that intact proteins are used, which circumvents any ambiguity or artifact that might arise from the use of peptides or fragments. Successful applications of this approach include the identification of photo-cross-linking between TnC residues 12 and 89 to TnI residues 130−134 and 108−113, respectively (*20*), TnC residue 158 to TnI residue 21 (*23*), TnC residue 98 to TnI residues 103−110 (*24*), and TnC residue 57 to TnI residues 113−121 (*25*).

The choices of residue 48 in the linker between helices B and C and residue 82 on helix D were governed by the following considerations: From the crystal structure of TnC, it can be seen that these resides are located near the entrance and on the opposite sides of the hydrophobic pocket. Previous studies on a TnC mutant containing both cysteines at these sites showed a remarkably high tendency to form a disulfide bond between these two cysteines (*16*). We reasoned that a photo-cross-linker that is attached at either site is likely to point into the hydrophobic pocket and therefore has a high probability of forming a photo-cross-link with the TnI segment interacting with the hydrophobic pocket.

We indeed found high yields of photo-cross-linking with TnI for both TnC mutants, in the TnC·TnI binary complex, the TnC·TnI·TnT ternary complex, and the Tn·Tm·F-actin reconstituted thin filaments. For the synthetic thin filaments, the extent of cross-linking was found to be significantly reduced in the absence vs the presence of Ca^{2+}. For both mutants, the site of cross-linking in TnI was identified to be Met121, five residues beyond the C-terminus of the inhibitory segment of TnI. The structural and functional implications of these findings will be discussed in conjunction with relevant findings by others.

MATERIALS AND METHODS

Chemicals. All reagents were of the highest grade commercially available. Common reagents were from Sigma. Reagents for reduction and alkylation were as follows: acrylamide from Bio-Rad (Hercules, CA), dithiothreitol from Calbiochem (La Jolla, CA) or Sigma, urea from Pierce (Rockford, IL) or United States Biochemical (Cleveland, OH), iodoacetamide from Sigma, and benzophenone-4-iodoacetamide (BP-IA) from Molecular Probes (Eugene, OR). For digestions: CNBr was from Pierce, modified trypsin from Promega (Madison, WI), and hydrogenated Triton X-100 from Calbiochem. The matrix α-cyano-4-hydroxycinnamic acid for MALDI-TOF mass spectrometry was from Sigma. All chemicals for automated Edman degradation sequencing were from Applied Biosystems/Perkin-Elmer. Water and acetonitrile for HPLC separations were from EM Science (Gibbstown, NJ).

Protein Preparations and Labeling. Skeletal Tn subunits (*26*) and Tm (*27*) were purified from rabbit skeletal muscle according to established methods. Rabbit skeletal F-actin (*28*) and myosin (*29*) were prepared as described previously. The latter was stored in 50% glycerol at −20 °C. Chymotryptic S1 was prepared from purified myosin according to Weeds and Taylor (*30*) and stored at −80 °C with 4 mg of sucrose/mg of S1 following additional purification on a Sephadex G-75 gel-filtration column.

Single-cysteine TnC mutants, TnC48 and TnC82, were constructed by converting Cys98 to Ser and Gln48 or Gln82 to Cys using previously described expression and purification procedures (*31*). A single-cysteine TnI mutant, TnI133, was made as described previously (*32*).

The engineered cysteines on TnC48 and TnC82 were alkylated with the bifunctional photoactivatable reagent BP-IA using a previously described procedure (*33*) except that the buffer solution contained 10 mM HEPES, pH 7.5, 0.1 M NaCl, and 2 mM EDTA; the concentrations of TnC and BP-IA were about 40 and 400 μM, respectively. To remove excess BP-IA, the labeled TnC samples were dialyzed against a solution containing 10 mM HEPES, 0.1 M NaCl, 1 mM DTT, and 0.2 mM $CaCl_2$ (buffer C), and stored at −20 °C if not used immediately. Solutions were shielded from light during the labeling and storage. The concentration of TnC after labeling was determined using the BCA Protein Assay Reagent (Pierce, Rockford, IL). The reagent was standardized with unlabeled TnC whose concentration had been spectrophotometrically determined. The typical efficiency of the labeling was >90%.

The cysteine on TnI133 was labeled with the fluorescence probe CP-Mal using a procedure described previously (*32*). Labeling of actin with CP-Mal was carried out as follows. Depolymerized actin, ~30 μM, in G-actin buffer containing 2 mM Tris-HCl, pH 8.0, 0.2 mM $CaCl_2$, 0.2 mM ATP was incubated with 150 μM CP-Mal overnight on ice. Following the removal of the undissolved probe by centrifugation, the actin solution was polymerized by the addition of 1 mM $MgCl_2$ and 50 mM NaCl. The F-actin was pelleted by high-speed centrifugation (Beckman TL100, 300000*g* for 30 min), leaving the majority of the excess probe in the supernatant. The actin pellets were dissolved in G-actin buffer that was one-fourth of the original volume, and the solution was dialyzed against 2L of G-actin buffer for 6−12 h. Following another high-speed centrifugation and before the final polymerization, the concentrations of actin and the fluorescence probe were determined by the absorbances at 280 nm [$\epsilon_{280} = 1.09$ (mg/mL)$^{-1}$ cm^{-1}] and 387 nm ($\epsilon_{387} = 29\,700$ M^{-1} cm^{-1}), respectively. The typical efficiency of labeling was 80−90%.

Reconstitution of the Binary and Ternary Tn Complexes, and Regulated Thin Filaments. The labeled TnC mutant, BP-TnC48 or BP-TnC82, was combined with skeletal TnI (binary complex) or TnI and TnT (ternary complex) in equimolar ratio in a denaturing solution containing 4 M GdmCl, 10 mM HEPES, pH 7.5, 0.1 M NaCl, and 2 mM EDTA. The protein complexes were renatured by dialysis against buffer C. To reconstitute the regulated thin filament, the reconstituted Tn complex was mixed with Tm and F-actin; the final concentrations were 6 μM Tn and Tm, and 42 μM F-actin. The mixtures were then dialyzed against F-actin buffer containing 2 mM Tris, pH 8.0, 50 mM NaCl, 0.2 mM $CaCl_2$, 1 mM $MgCl_2$, 0.2 mM ATP, and 0.5 mM DTT.

Photo-Cross-Linking. Before UV irradiation, the stock solution of each mixture was split into four aliquots of about 100 μL each; one was saved as the unirradiated control, and three were used to examine photo-cross-linking in different metal ion states. The apo or Mg^{2+} states were attained by adding 2 mM EDTA, or 2 mM EGTA and 8 mM $MgCl_2$, respectively. Following UV irradiation in borosilicate glass tubes for 25 min, unless otherwise indicated, the photo-cross-linking patterns were analyzed using SDS−PAGE (12.5% acrylamide). In the cases that quantitative analysis was desired, the gels were scanned with a UMAX Super Vista S-12 scanner and the intensities digitized with the program NIH Image.

Acto-S1 ATPase Assays. Ternary Tn complexes containing the appropriate subunits were reconstituted and exposed to UV, if desired, as described above. At the time of assay, the ternary complexes were mixed with Tm and actin to final concentrations of 0.6 μM Tn and Tm, 3.0 μM F-actin. The final salt concentration was about 20 mM NaCl. $CaCl_2$ (0.2 mM), or EGTA (2 mM) plus $MgCl_2$ (5 mM) was present in the assays for the activated or the inhibited condition, respectively. The ATPase reactions were initiated by the addition of 1.5 μM S1. Photometric determination of the phosphate-release time course was carried out as described previously (*33*).

Purification of the Cross-Linking Products. The binary complexes of BP-TnC48·TnI and BP-TnC82·TnI were made as described above. For the former, one portion was irradiated in the presence of Ca^{2+} (in buffer C), the other in the absence of Ca^{2+} (buffer C plus 2 mM EGTA and 8 mM $MgCl_2$). BP-TnC82·TnI was irradiated in the presence of Ca^{2+} only. The components of each sample were separated on an anion exchange column, Mono Q HR 5/5 (Pharmacia), using a Waters 650E FPLC system (Millipore). The column was equilibrated with a buffer containing 6 M urea, 0.1 M NaCl, 20 mM Tris-HCl, pH 8.0, 2 mM DTT before the samples were loaded. The proteins were eluted with a salt gradient from 0.1 to 0.6 M NaCl in the same buffer with a flow rate of 0.7 mL/min. The eluate was monitored with a UV absorption detector at 280 nm. The peaks were identified by SDS−PAGE. Free TnI, cross-linked TnI and TnC, and free TnC were eluted at 0.1, 0.33, and 0.35 M NaCl, respectively. The fractions containing the cross-linking product were pooled and dialyzed against 2 mM NH_4HCO_3 and lyophilized thereafter. The purified cross-linking products are referred to as BP-C48-I and BP-C82-I, respectively.

Alkylation of TnI. Cysteine residues in TnI were alkylated with acrylamide to form the *S*-β-propionamide cysteine derivative (*39*). Rabbit skeletal TnI (50 nmol), BP-C82-I (10 nmol), and BP-C48-I (10 nmol) were dissolved in 100 μL of a solution containing 10 mM DTT, 0.25 M Tris-HCl, 1 mM EDTA, 6 M urea and incubated at 60 °C for 30 min. The samples were incubated at 37 °C for 2 h following the addition of 50 μL of 6 M acrylamide, and were then directly desalted on a 4.6 mm × 25 cm Vydac (214TP54) C_4 column using a Hewlett-Packard 1090 M HPLC system.

BP-C48-I cross-linked in the absence of Ca^{2+} was alkylated with iodoacetamide by dissolving the sample in 25 μL of a solution containing 8 M urea and 100 mM NH_4HCO_3, followed by the addition of 5 μL of 45 mM DTT and incubation at 50 °C for 15 min. The sample was allowed to cool to room temperature after which 5 μL of 100 mM iodoacetamide was added. The reaction was allowed to proceed for 15 min before dilution with 60 μL of water.

Chemical and Enzymatic Cleavage of BP-TnC82-I. The alkylated BP-C82-I sample was dissolved in 50 μL of 70% formic acid, and 2 mg of CNBr freshly dissolved in 5 μL of 70% formic acid was added. The sample was incubated at room temperature in the dark for 18 h, then diluted to 0.5

mL with water, and dried in a SpeedVac concentrator. The sample was redissolved in 25% TFA prior to injection onto an HPLC. CNBr peptides were separated with a 2.1 mm × 25 cm Vydac (218TP52) C_{18} column using a linear gradient from 100% solvent A (0.1% TFA) to 70% solvent B (0.08% TFA in acetonitrile/water, 70/30) in 70 min at a flow rate of 210 μL/min. The eluate was monitored with a Hewlett-Packard UV diode array detector at 210 (for peptides) and at 260 and 300 nm (for BP), and fractions were collected manually.

Fractions identified as being cross-linked peptides from the CNBr digestion mixture were further broken down by trypsin digestion. CNBr peptide fractions were dried down and redissolved in 50 μL of a digestion buffer containing 100 mM $NaHCO_3$, 10% acetonitrile, 1% hydrogenated Triton X-100, pH 8.2; 2 μg of trypsin in 4 μL of 50 mM acetic acid was added to the samples. They were then incubated at 37 °C overnight and injected directly into the HPLC. Tryptic peptides were separated on a 1 mm × 25 cm Applied Biosystems (Aquapore RP-300) C_8 column using a linear gradient from 100% solvent A to 55% solvent B in 30 min and then 55% solvent B to 85% solvent B in 10 min at a flow rate of 150 μL/min. The eluate was monitored at 210, 260, and 300 nm, and fractions were collected manually.

Enzymatic Cleavage of BP-C48-I. BP-C48-I prepared in the presence of Ca^{2+} and alkylated with acrylamide was dissolved in 25 μL of an 8 M urea, 100 mM NH_4HCO_3 solution and then diluted with water to make the final concentration of urea 2 M. Trypsin (1 μg) in 4 μL of 50 mM acetic acid was then added, and the sample was incubated at 37 °C overnight. BP-C48-I cross-linked in the absence of Ca^{2+} and alkylated with iodoacetamide was digested by trypsin with the same procedure immediately following the alkylation. The tryptic peptides were separated with a 2.1 mm × 25 cm Vydac (218TP52) C_{18} column as described above.

Protein Sequencing, Mass Spectrometry, and HPLC. Automated Edman degradations were performed on an Applied Biosystems/Perkin-Elmer 494 Procise sequencing system. MALDI-TOF mass spectrometry was performed on a Perseptive Biosystems Linear Voyager BioSpectrometry Workstation. HPLC was performed on a Hewlett-Packard 1090 M HPLC system equipped with a UV photodiode array detector.

RESULTS

Photo-Cross-Linking. In the TnC·TnI binary complex, BP-TnC48 was photo-cross-linked to TnI with high yield both in the presence and in the absence of Ca^{2+} (Figure 1A) indicated by a protein band above TnC and TnI on the SDS gel. This band is absent in the unirradiated sample. The yield of photo-cross-linking was slightly reduced in the absence of Ca^{2+}.

In the TnC·TnI·TnT ternary complex, BP-TnC48 predominantly photo-cross-linked with TnI under all the tested metal ion conditions (Figure 1A). The yields were nearly Ca^{2+}-independent and comparable to those in the binary complex. Some photo-cross-linking with TnT, appearing as two separate bands above the BP-C48-I band, was observed in the presence of Ca^{2+} but not in its absence. The yield of the BP-C48-T cross-linking was much lower compared to

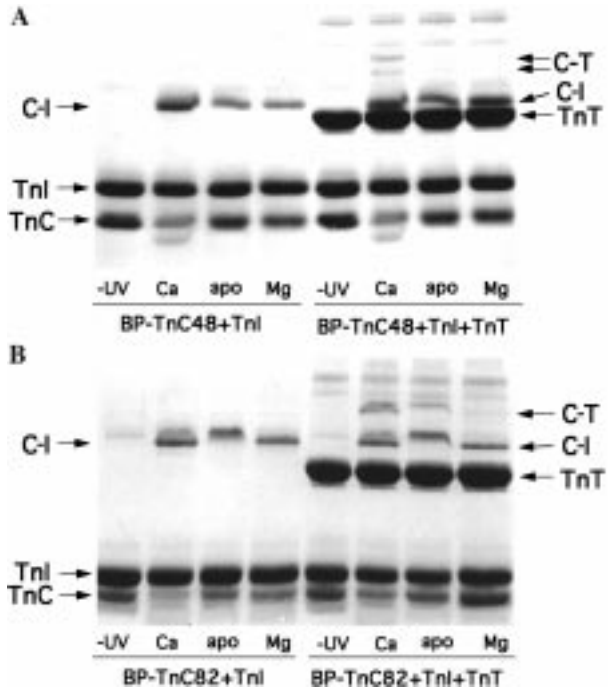

FIGURE 1: Photo-cross-linking of TnC mutants in the binary and ternary complexes. BP-TnC48 (A) and BP-TnC82 (B) were recombined with TnI (left four lanes) or TnI and TnT (right four lanes) and dialyzed against a solution containing 10 mM HEPES, pH 7.5, 0.1 M NaCl, 0.2 mM $CaCl_2$. Aliquots of the samples in the above medium (lanes Ca), with 2 mM EDTA (lanes apo), or with 2 mM EGTA and 8 mM $MgCl_2$ (lanes Mg) were irradiated with UV light. An unirradiated sample (lanes −UV) was used as control. On these Coomassie Blue stained SDS gels, the TnC−TnI cross-linking products appear above TnT, and the TnC−TnT cross-linking products are above the cross-linked TnC-TnI bands.

that of BP-C48-I. These two BP-C48-T bands obtained with the ternary complex were of the same mobilities on the SDS gel as those obtained with the binary complex of BP-C48·T (data not shown).

In both the binary and ternary complexes, but only in the presence of Ca^{2+}, a band of higher mobility than that of BP-TnC48 appeared upon irradiation (the lowest bands in lanes "Ca" of Figure 1A). The same band was obtained when uncomplexed BP-TnC48 was irradiated (data not shown). It most likely corresponds to an internally cross-linked TnC species whose mobility on the SDS gel is enhanced owing to its more compact structure.

The cross-linking results for BP-TnC82 are similar to those for BP-TnC48 with minor differences: BP-TnC82 photo-cross-linked to TnI in both the TnC·TnI and the TnC·TnI·TnT complexes with similar yields and with little Ca^{2+} dependence (Figure 1B). Photo-cross-linking of BP-TnC82 to TnT produced a single band on the SDS gel in both the TnC·TnT (data not shown) and the TnC·TnI·TnT complexes (Figure 1B). The yield of BP-C82-T was significantly lower in the presence of Mg^{2+} than in the presence of Ca^{2+}. There was no indication of any intra-TnC photo-cross-linking under any condition.

In the case of reconstituted Tn·Tm·actin thin filaments, either actin or TnI was labeled with the fluorescent probe CP-Mal to facilitate the identification of the cross-linking bands. No photo-cross-linking of BP-TnC48 or BP-TnC82 with actin was observed (data not shown). Photo-cross-linking with CP-TnI was indicated by the presence of

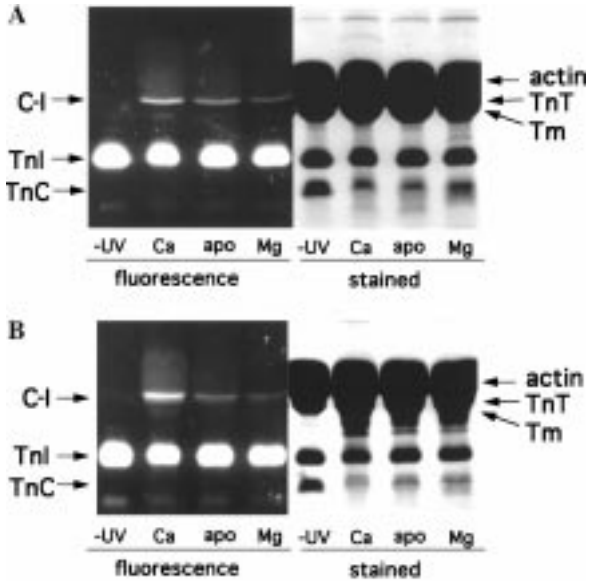

FIGURE 2: Photo-cross-linking of TnC mutants in reconstituted thin filaments. Ternary Tn complexes containing BP-TnC48 (A) or BP-TnC82 (B) and CP-TnI133 were reconstituted in the same solution as that in the legend for Figure 1. They were then combined with Tm and F-actin to the following final concentrations: 42 μM F-actin, 6 μM Tm and Tn; and dialyzed against a solution containing 2 mM Tris-HCl, pH 8.0, 50 mM NaCl, 0.2 mM ATP, 0.2 mM $CaCl_2$, 1 mM $MgCl_2$, and 0.2 mM DTT. The lane designations are the same as in Figure 1. The gels were first photographed with UV excitation (left panels) and then stained with Coomassie Blue (right panels). The only cross-linking found was between TnC and TnI, observable only on fluorescence pictures. On the stained pictures the corresponding bands overlap the bands of actin which was in manyfold excess.

fluorescent bands in the same positions as those derived from photo-cross-linking in the binary and the ternary complexes (Figure 2). Note that these bands could not be detected on the Coomassie Blue stained gels because their electrophoretic mobility is similar to that of actin which was in large excess. Although the fluorescence intensities of the cross-linked BP-TnC48 or BP-TnC82 with CP-TnI were low, probably due to absorption by actin, it is evident that the yield was higher in the presence of Ca^{2+} compared with that in its absence. All the samples were centrifuged following UV irradiation, and the supernatants and the pellets were examined on SDS gels. All thin filament components, including the cross-linked TnC and TnI, were pelleted with F-actin in the presence and absence of Ca^{2+} (data not shown), confirming that the photo-cross-linking within the Tn complex occurred while attached to thin filaments.

Regulatory Activities. The regulatory activities of the Tn complexes reconstituted with the labeled or unlabeled mutant TnC's were tested. The irradiated or unirradiated Tn complexes were added to Tm and actin. The ATPase activities of myosin S1 in the presence of these reconstituted thin filaments were then assayed. The results are summarized in Table 1. Without irradiation, the activities in the presence and the absence of Ca^{2+} for samples that contain either unlabeled or labeled TnC mutants were similar to those for the control sample, which contained rabbit skeletal TnC. The inhibited activities were approximately 15% of those in the presence of Ca^{2+} (the slightly higher activities for the labeled TnC's may be due to inaccuracies in concentration determinations after labeling). These results indicate that neither the mutations nor the labeling affected the regulatory activities of these TnC's.

Table 1: Tm−Acto-S1 ATPase Activities Regulated by Tn Reconstituted with Different Forms of TnC

	−UV		+UV[a]	
troponin containing	$+Ca^{2+}$	$-Ca^{2+}$	$+Ca^{2+}$	$-Ca^{2+}$
TnC	100[b]	15	102	14
TnC48	112	16	109	14
TnC82	95	15	97	15
BP-TnC48	116	22	105	40
BP-TnC82	114	20	113	42

[a] UV irradiation (20 min) was performed on Tn ternary complexes prior to mixing with actin and Tm. [b] All activities are expressed in percent. 100% represents 0.52 μmol of P_i·(mg of S1)$^{-1}$·min^{-1}. Assay conditions: 1.5 μM S1, 3 μM F-actin, 0.6 μM Tm, 0.6 μM Tn, 10 mM HEPES, pH 7.5, 20 mM NaCl, 5 mM $MgCl_2$, 2 mM DTT, 1.5 mM ATP, and 0.2 mM $CaCl_2$ for the $+Ca^{2+}$ state or 2 mM EGTA for the $-Ca^{2+}$ state, at 25 °C.

After 25 min of UV exposure, the ATPase activities with or without Ca^{2+} with Tn's that contained unlabeled TnC mutants showed no change compared with the unirradiated samples, indicating that UV light itself does not change the properties of Tn. For the samples containing BP-TnC48 or BP-TnC82, the activities in the presence of Ca^{2+} were unaffected by irradiation. The activities in the absence of Ca^{2+}, on the other hand, were significantly higher for the irradiated samples than for the unirradiated controls, indicating that the inhibitory activities of these Tn's were impaired by virtue of the photo-cross-linking. Although the loss of inhibition was not total, one should keep in mind that the cross-linking was also incomplete (Figure 1).

Determination of the Cross-Linking Site on TnI for BP-C48-I. It has been noted from previous cross-linking work with TnC (*34*) that the CNBr peptide 46−78 was not recovered by reverse-phase HPLC. Oftentimes a change of a single amino acid in the sequence of a peptide dramatically changes its solubility. Since a tryptic digest generates a C-terminal Arg for peptide 45−81, it would in theory produce a slightly more basic peptide with properties which could enhance its solubility in the acidic solvent system used for peptide isolation. Thus, BP-C48-I was digested with trypsin in this work. The analysis by HPLC of the BP-TnC48 tryptic digest shows that the labeled TnC peptide (residues 45−81) elutes almost at the end of the gradient, reflecting the interesting solubility properties of this region of TnC (Figure 3). The arrows in Figure 3 indicate the well-defined A_{260} fractions in the digest of BP-C48-I which were not found in the un-cross-linked controls. These fractions were analyzed by both mass spectrometry and protein sequencing. Sequence analysis of the cross-linked fraction eluted at 42.5 min showed the presence, in exactly 1:1 molar ratio, of TnC (residues 45−52) and TnI (residues 116−123), among which Met121 of TnI had a very low yield indicating that it is the most cross-linked residue (Table 2).

To gain further support for the notion that the two peptides of TnC and TnI were cross-linked, we performed MALDI-TOF mass spectroscopic analysis. It produced a mass of 1954.8 Da for this fraction which is exactly the sum of TnC 45−52 (850.1 Da), the cross-linker (238 Da), and TnI 116−123 (866.1 Da) (Figure 4A). The fraction that eluted at 68.5 min was also examined. Sequence analysis showed the

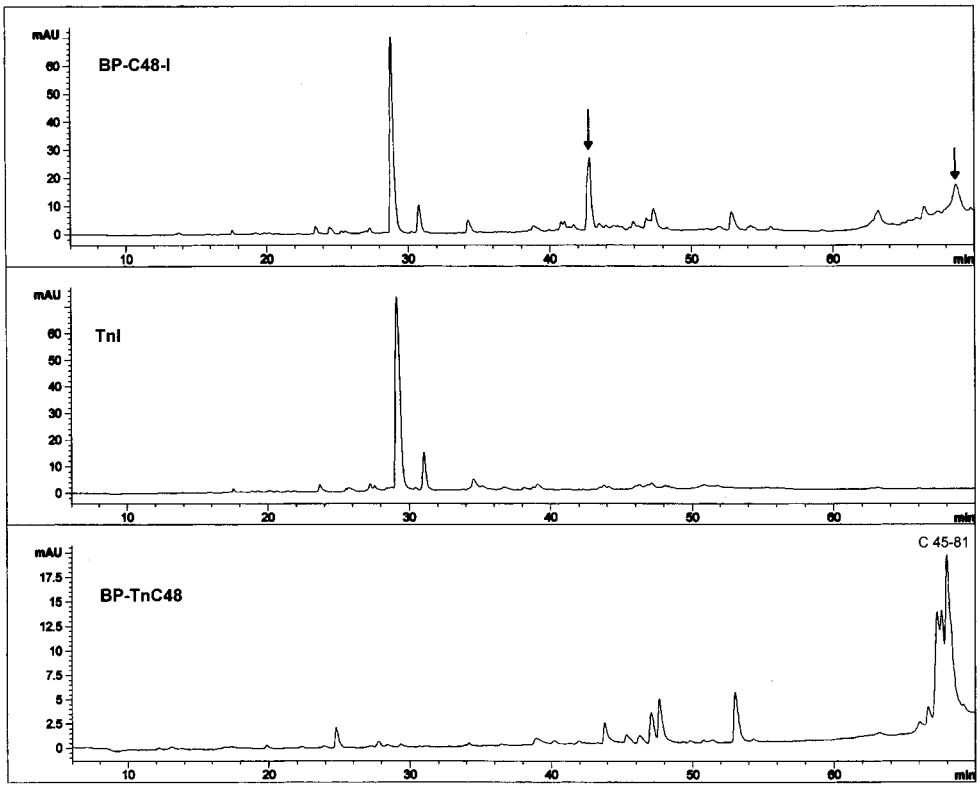

FIGURE 3: Reverse-phase HPLC separation of tryptic digests monitored at 260 nm. The tryptic digests of BP-C48-I (top panel), TnI (middle panel), and BP-TnC48 (bottom panel) were fractionated using a Vydac (218TP52) C_{18} column. The elution positions of the cross-linked peptides are indicated by arrows in the BP-C48-I digest. Also indicated is the elution position of the BP-TnC48 tryptic peptide 45−81 (bottom panel). Strong absorbance at 260 nm is indicative of cross-linked peptides. The absorbance at 260 nm found in the TnI digest is due to the tryptophan absorbance of TnI tryptic peptides.

Table 2: Yields of Edman Sequence Analysis in Picomoles for Cross-Linked Peptides Derived from the Tryptic Fractions of BP-C48-I and BP-C82-I

	BP-C48-I				BP-C82-I[a]	
	5267 Da		1954.8 Da		1177 Da TnI	1159 Da TnI
Cycle	TnC (45−81)	TnI (116−123)	TnC (45−52)	TnI (116−123)	(117−123)	(117−123)
1	M 131	M −	M 122	M −	S 10	S 8
2	L 85	S 43	L 73	S 35	A 14	A 9
3	G 63	A 67	G 54	A 50	D 13	D 5
4	X[b] −	D 80	X −	D 33	A 12	A 7
5	T 46	A 68	T 51	A 50	M 0.4	M 0.1
6	P 33	M 15	P 39	M 15	L 12	L 7
7	T 26	L 51	T 27	L 45	K 9	K 5
8	K 73	K −	K 78	K −		
9	E 44					
10	E 53					
11	L 44					
12	D 26					
13	A 23					
14	I 31					
15	I 41					

[a] Yields are not reported for the TnC Cys-Hse peptide. [b] Denotes site of cross-linking which showed no PTH derivative.

presence of peptides of TnC (45−81) and of TnI (116−123) in an equimolar ratio (Table 2). This would arise from incomplete tryptic cleavage at Lys52 of TnC. Again in the sequence analysis of this fraction Met121 of TnI occurred in very low yield relative to other TnI residues. A mass of 5267 Da for this fraction is in excellent agreement with the sum of the masses of TnC 45−81 (4163.7 Da), the cross-linker (238 Da), and TnI 116−123 (866.1 Da) equalling 5267.8 Da (Figure 4B).

The BP-C48-I complex prepared in the absence of Ca^{2+} was also examined. The tryptic peptide maps were almost identical to that obtained in the presence of Ca^{2+}. Again the cross-linked fractions eluted at 42.5 and 68.5 min showed the same masses of 1954 and 5267 Da, respectively. Sequence analysis of the fraction at 68.5 min showed peptides of TnC 45−81 and TnI 116−123 in equimolar ratio with, again, Met121 of TnI at a level as low as 25% of that expected.

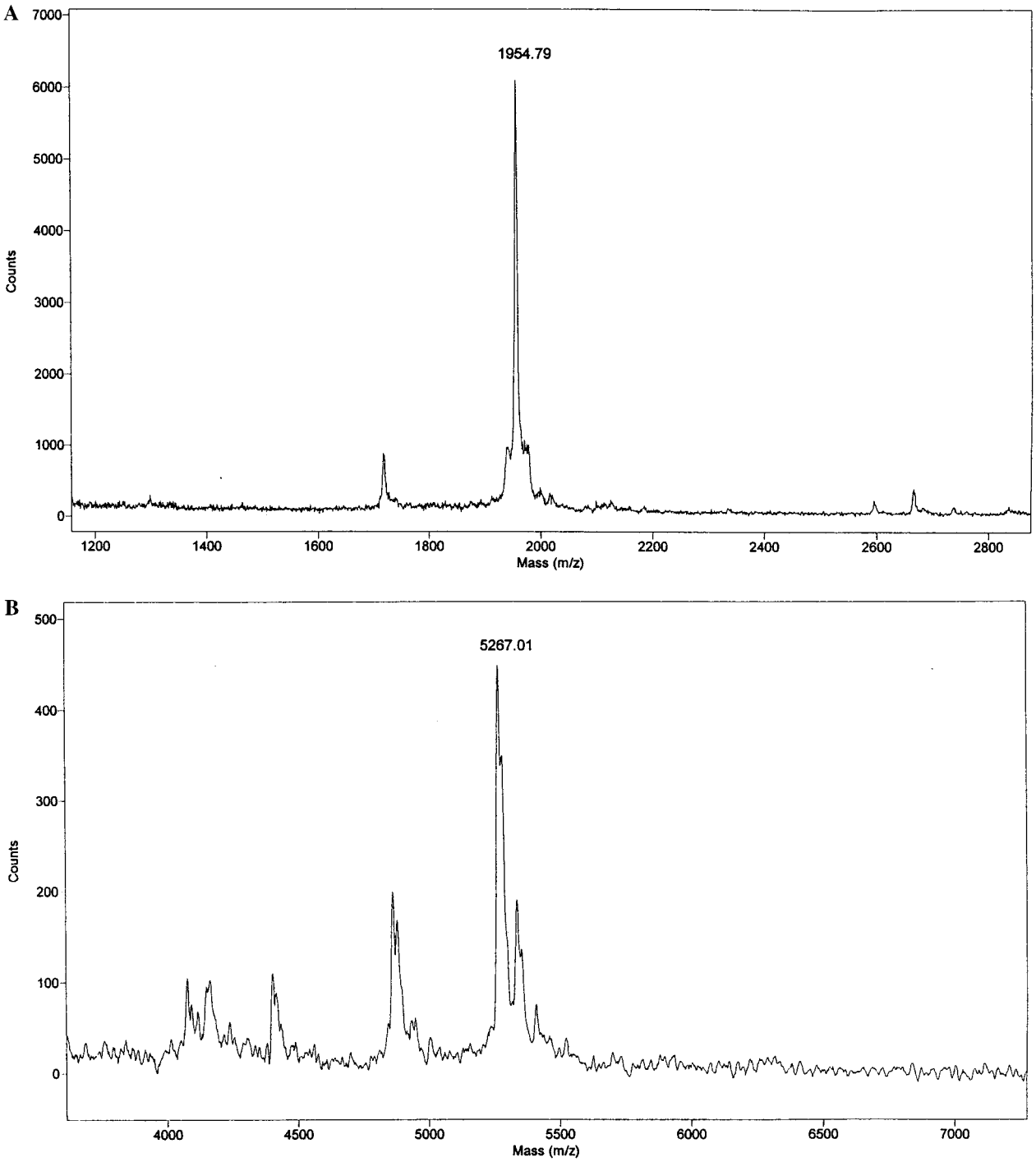

FIGURE 4: MALDI-TOF mass spectra for cross-linked peptides. The mass of the peptide in the fraction eluted at 42.5 min (A) and 68.5 min (B) in the top panel of Figure 3 was determined by mass spectrometry. The masses at 1954.8 and 5267 Da represent singly protonated cross-linked peptides (see text).

Determination of the Cross-Linking Site on TnI for BP-C82-I. BP-C82-I was digested with CNBr. Comparison of the CNBr digest of BP-C82-I with that of BP-TnC82 and TnI showed a somewhat broad heterogeneous cross-linked peptide eluting between 49 and 53 min (Figure 5). Sequence analysis of this fraction showed several sequences (data not shown). The two major sequences were the expected peptide of TnC (residues 80−83) and a TnI peptide (residues 117−134), which appeared in nearly equimolar amounts. Other sequences amounted to 30−50% of the major sequences. The fact that Met121 in TnI peptide (117−134) was not digested by CNBr suggests that the residue had been modified, likely by cross-linking. The presence of the minor sequences may be a matter of simple coelution of partially cleaved CNBr peptides. Mass spectrometry was not useful owing to this heterogeneity.

To delineate more precisely the site of cross-linking, the CNBr fraction for the cross-linked peptide was further digested with trypsin (Figure 6). The digest was eluted with five closely spaced A_{260} peaks (bottom panel of Figure 6). These fractions were evaluated by MALDI-TOF mass analysis and found to have masses of 1177 Da for the 22.5 min fraction and 1159 Da (loss of one water) for the 26 min fraction (Figure 7), respectively. Sequence analysis of these

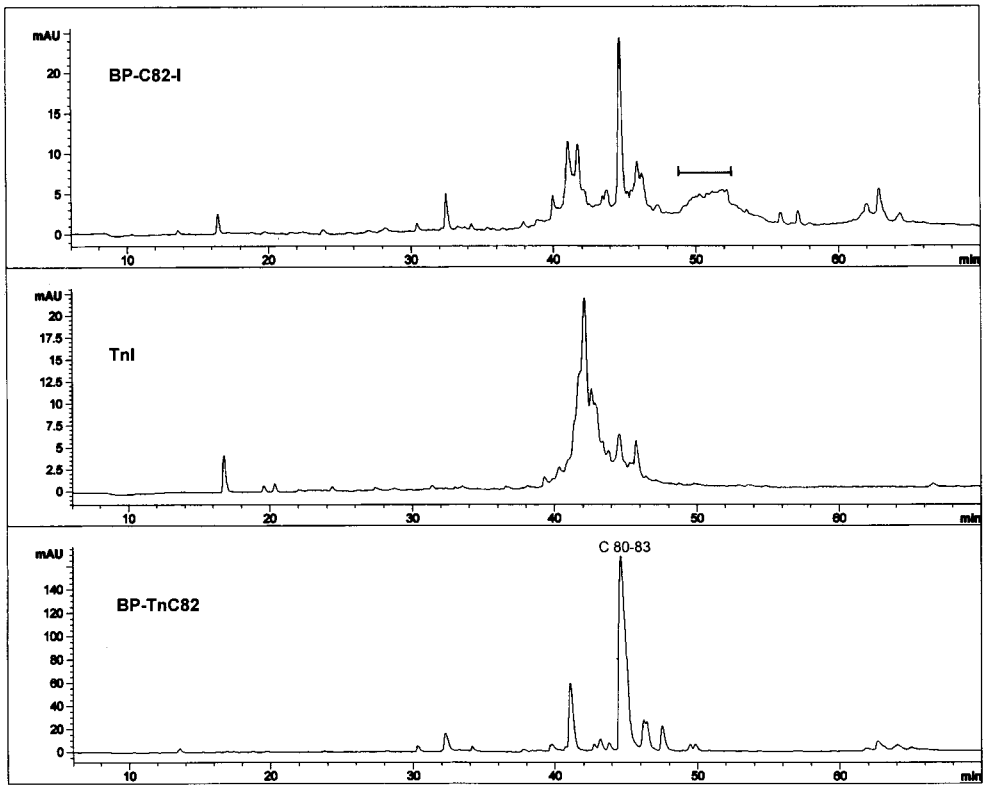

FIGURE 5: Reverse-phase HPLC separation of CNBr digests monitored at 260 nm. The CNBr digests of BP-C82-I (top panel), TnI (middle panel), and BP-TnC82 (bottom panel) were separated on a Vydac (218TP52) C_{18} column. The elution positions of the cross-linked peptides were found between 49 and 53 min and indicated by a bar. Also indicated is the elution position of BP-TnC82 CNBr peptide, 80−83 (bottom panel). The strong 260 nm absorbance found in the TnI digest is due to tryptophan absorbance of TnI CNBr peptides.

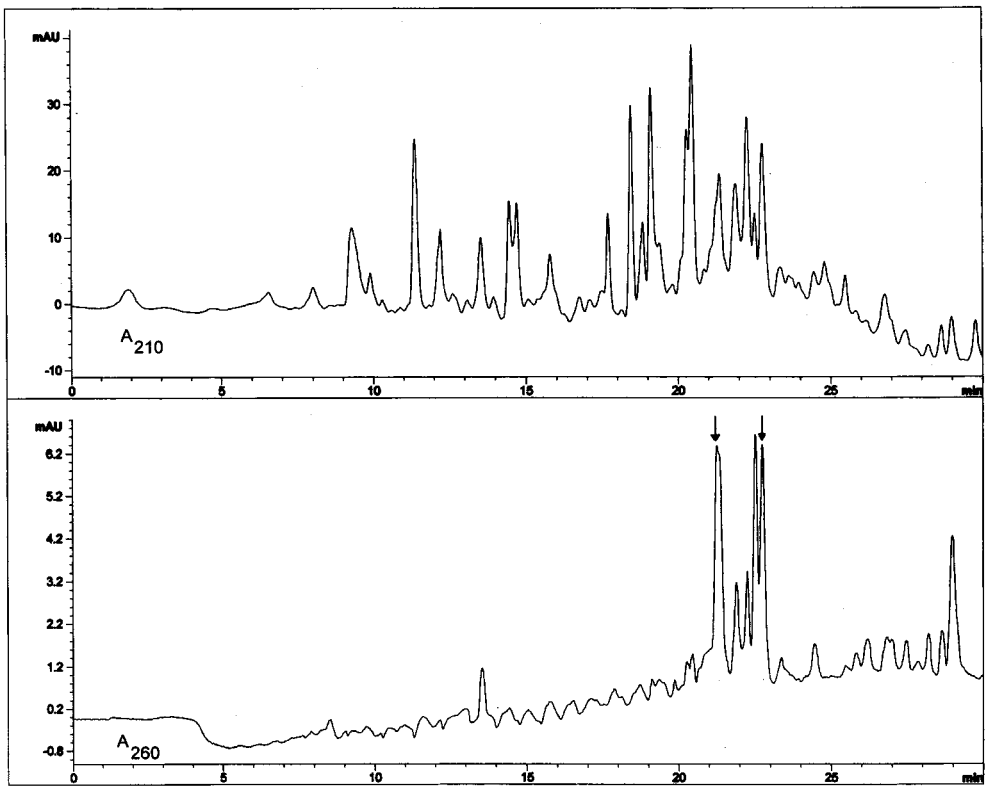

FIGURE 6: Reverse-phase HPLC separation of tryptic digests monitored at 210 and 260 nm. The CNBr fraction of BP-C82-I found between 49 and 53 min in Figure 6 was further digested with trypsin. The tryptic peptides were separated on an Aquapore RP-300 C_8 column. Absorbances at 210 and 260 nm (indicative of cross-linked peptides) are shown in the upper and lower panel, respectively. The arrows indicate the fractions that were subjected to mass spectrometry analysis.

two fractions showed one common sequence derived from TnI (SADAXLK) which corresponds to residues 117−123. The expected TnC peptide CHse (residues 82−83) was also present, but the yield of Hse was not quantitative enough to

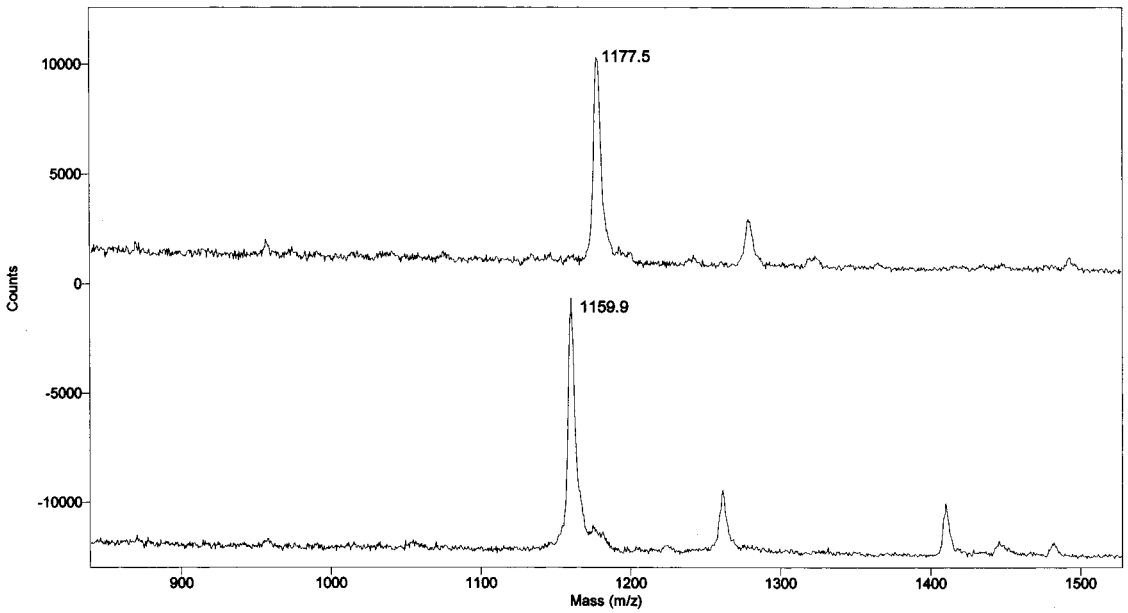

FIGURE 7: MALDI-TOF mass spectra of the cross-linked peptides shown in Figure 6. The top spectrum showing a singly protonated peptide mass of 1177.5 Da and the bottom spectrum showing a mass of 1159.9 Da represent the fractions found at 22.5 and 26 min, respectively, in Figure 6. Both fractions were identified as the same cross-linked peptide (see text for details).

be used to determine the relative yields (Table 2). However, the mass spectrometry data supported the presence of the TnC peptide (CHse lactone), 204.3 Da; the cross-linker, 238 Da; and a TnI peptide (SADAMLK), 735 Da, totaling 1177.3 Da. In the sequence analysis of these fractions the yield of Met121 of TnI was negligible, again indicating that it was the most cross-linked residue. The presence of the 1159 Da fraction was probably due to the loss of water from the cross-linker since the homoserine is presumably in its lactone form in the 1177.3 Da fraction. The exact nature of how water could be lost from the benzophenone cross-linker is not understood.

DISCUSSION

The major aim of this work was to determine which region of TnI interacts with the hydrophobic patch of TnC, the area that becomes exposed on binding of Ca^{2+} to the N-terminal triggering sites. Our cross-linking results show that, in both the binary TnC·TnI complex and the intact ternary Tn complex, photo-cross-linkers attached to both residues 48 and 82 of TnC indeed cross-link primarily to TnI with roughly equal efficiency. TnC residues 48 and 82 are located at the rim of the N domain hydrophobic pocket on the B, the C, and the D helix side, respectively. If they cross-link to the same region in TnI, that region is very likely to be between the B, C, and D helix, i.e., inside the N-terminal domain hydrophobic pocket of TnC when it is open.

Our microsequencing and mass spectrometric studies have identified one single photo-cross-linking site in TnI, viz., Met121, in the complex with either BP-TnC48 or BP-TnC82. This shows unequivocally that the region in TnI that interacts with the N-domain hydrophobic patch of TnC contains this residue. The residues adjacent to Met121 in the sequence AMLKALLG (residues 120−127) are highly hydrophobic, making this TnI segment the prime candidate for interaction with TnC's N-domain hydrophobic pocket. This region is not the inhibitory region (residues 96−115) that is believed to switch back and forth between TnC and actin upon the activation and inhibition of muscle contraction.

This result for the complex of intact TnC and TnI is in harmony with many studies using fragments or peptides. For example, affinity chromatography studies revealed that TnI residues 116−131 enhanced the affinity of the inhibitory region for TnC in a Ca^{2+}-dependent manner (*21*). Based on fluorescence titration and sequence analysis studies, it was concluded that the second of three roughly homologous sequences in the C-terminal half of TnI (residues 121−132, termed the β motif) interacts with the N-terminal domain of TnC (*35*). More direct evidence is provided by an NMR study using a truncated TnC (N-terminal domain only) and the TnI peptide 115−131. The chemical shifts of backbone amides at TnC residues that are near or at the hydrophobic patch (e.g., 42, 46, 49, and 50 on the B helix; and 82 on the central D helix, where the numbers refer to chicken skeletal TnC sequence) were significantly changed by the addition of the TnI peptide with saturating Ca^{2+} (*22*). Recently, the crystal structure of TnC complexed with the N-terminal peptide of TnI, residues 1−47, has been solved (*36*). This structure reveals that the TnI segment 3−33 is an α-helix lying in the open hydrophobic pocket formed by helices E, F, and G in the C-terminal domain of TnC. These authors also modeled the interaction of the TnI 96−127 region with TnC's N-terminal domain. In their model, residues 114−126 interact strongly with the exposed N-terminal hydrophobic patch. Most interestingly, Met121 of TnI was indicated as one of the key residues in the contact.

In the synthetic thin filaments, for both BP-TnC48 and BP-TnC82, we found that the extent of TnC−TnI cross-linking was clearly Ca^{2+}-sensitive, being significantly reduced in the absence (Mg^{2+} state) than in the presence of Ca^{2+} (Ca^{2+} state) (Figure 2). This suggests that residue 121 of TnI and the residues adjacent to it move away from the N-terminal hydrophobic patch of TnC in response to its closing when Ca^{2+} is absent. This movement, however,

cannot be very large because some photo-cross-linking could still be observed (Figure 2). This small movement can nevertheless trigger larger movements of the N-terminal end of the inhibitory region, and of the 128−148 region toward actin.

It is curious, however, that no Ca^{2+} sensitivity was observed in the binary TnC·TnI and the ternary TnC·TnI·TnT complexes. We interpret these observations as follows: in the binary and ternary complexes, this movement of TnI's residue 121 may be nonexistent or so small that it cannot be detected by photo-cross-linking. In the reconstituted thin filament, on the other hand, owing to the large-scale movements of the aforementioned TnI regions toward actin, this movement of the Met121 region is accentuated and becomes apparent in our photo-cross-linking experiments.

That Tn behaves differently in the free state versus when it is incorporated into the thin filament is not unusual. For example, we have observed that the digestion of TnI by chymotrypsin is different for free Tn versus Tn in the reconstituted Tn·Tm·actin thin filament (*37*). Also, the Ca^{2+}-induced change in distance between residues 48 and 133 in the N- and C-terminal regions of TnI was only found in the thin filament state and not in free Tn (*33*).

The suggestion that this Met121-containing region of TnI, which is distinct from its inhibitory region, stays outside but very close to TnC's N domain hydrophobic pocket when the pocket is closed implies that this region does not directly participate in TnI's interaction with actin in the inhibited state of muscle. This is supported by some experimental results: in the Ca^{2+}-free state of thin filament, the benzophenone moiety attached to TnI residue 104 photo-cross-linked to actin with high yield, indicating that the N-terminal portion of TnI's inhibitory region interacts with actin under these conditions (*38*); in contrast, photo-cross-linking between TnI residue 121 and actin is undetectable under identical conditions.[2] Tripet et al. (*21*) have shown that if residues 116−139 of TnI are attached to the inhibitory peptide they even reduce the affinity of the inhibitory region to actin if the peptide is not extended further to residue 148.

It is interesting to note that for BP-TnC82, there is substantial photo-cross-linking to TnT, indicating that TnT is close to TnC (and perhaps TnI as well) near TnC's N-terminal hydrophobic pocket. Moreover, this photo-cross-linking is Ca^{2+}-sensitive, raising the possibility that this region of TnT is involved in the regulatory process.

From our studies on the regulatory activities of the various Tn preparations (Table 1), we found that for both BP-TnC48 and BP-TnC82 the photo-cross-link had no effect on the S1·Tn·Tm·F-actin ATPase activity in the presence of Ca^{2+}, but this activity in the absence of Ca^{2+} is not as low as that for the controls (∼41 vs ∼14%). This indicates that the photo-cross-link impairs the inhibitory activity of the Tn in the absence of Ca^{2+}. A possible mechanism for this impairment is that the photo-cross-link inhibits the aforementioned movement of the TnI Met121 region upon the closing of TnC's N-terminal hydrophobic patch. This would prevent the movement of other TnI regions toward actin and further events in the regulatory process. We noted, however, that the impairment was not complete; i.e., the ATPase activities in the absence of Ca^{2+} did not reach those in the presence of Ca^{2+}. This may be because the benzophenone moiety contains several flexible bonds, so that the cross-link is not completely rigid, and a slight movement of this region away from TnC can still take place. This may also be simply due to the fact that the photo-cross-linking was not complete, and without reliable methods to determine the extent of cross-linking this issue cannot be resolved at the present time. Future experiments using more rigid cross-linkers or disulfide cross-linking are underway in our laboratory.

In summary, the TnI region containing Met121 adjacent to the C-terminal end of TnI's inhibitory region has been identified as the partner of TnC's N-terminal domain hydrophobic pocket in constituting the core of the Tn Ca^{2+} switch. The signal of Ca^{2+} binding triggers the opening and closing of TnC's N domain hydrophobic pocket, which directs the movement of this TnI region in and out of the pocket. This, in turn, leads to a relatively large movement of other C-terminal TnI regions away from TnC and toward actin.

[2] Luo, Wu, Gergely, and Tao, unpublished results.

REFERENCES

1. Leavis, P. C., and Gergely, J. (1984) *CRC Crit. Rev. Biochem. 16*, 235−305.
2. Farah, C. S., and Reinach, F. C. (1995) *FASEB J. 9*, 755−767.
3. Zot, A. S., and Potter, J. D. (1987) *Annu. Rev. Biophys. Biophys. Chem. 16*, 535−559.
4. Tobacman, L. S. (1996) *Annu. Rev. Physiol. 58*, 447−481.
5. Sundaralingam, M., Bergstrom, R., Strasburg, G., Rao, S. T., Greaser, M., and Wang, B. C. (1985) *Science 227*, 945−948.
6. Herzberg, O., and James, M. N. G. (1985) *Nature 313*, 653−659.
7. Herzberg, O., and James, M. N. G. (1988) *J. Mol. Biol. 203*, 761−779.
8. Potter, J. D., and Gergely, J. (1975) *J. Biol. Chem. 250*, 4628−4633.
9. Robertson, S. P., Johnson, J. D., and Potter, J. D. (1981) *Biophys. J. 34*, 559−569.
10. Herzberg, O., Moult, J., and James, M. N. G. (1986) *J. Biol. Chem. 261*, 2638−2644.
11. Wang, Z., Gergely, J., and Tao, T. (1992) *Proc. Natl. Acad. Sci. U.S.A. 89*, 11814−11817.
12. Gagne, S. M., Tsuda, S., Li, M. X., Smillie, L. B., and Sykes, B. D. (1995) *Nat. Struct. Biol. 2*, 784−789.
13. Strynadka, N. C. J., Cherney, M., Sielecki, A. R., Li, M. X., Smillie, L. B., and James, M. N. G. (1997) *J. Mol. Biol. 273*, 238−255.
14. Houdusse, A., Love, M. L., Dominguez, R., Grabarek, Z., and Cohen, C. (1997) *Structure 5*, 1695−1711.
15. Fujimori, K., Sorenson, M., Herzberg, O., Moult, J., and Reinach, F. C. (1990) *Nature 345*, 182−184.
16. Grabarek, Z., Tan, R.-Y., Wang, J., Tao, T., and Gergely, J. (1990) *Nature 345*, 132−135.
17. Syska, H., Wilkinson, J. M., Grand, R. J. A., and Perry, S. V. (1976) *Biochem. J. 153*, 375−387.
18. Olah, G. A., and Trewhella, J. (1994) *Biochemistry 33*, 12800−12806.
19. Farah, C. S., Miyamoto, C. A., Ramos, C. H. I., da Silva, A. C. R., Quaggio, R. B., Fujimori, K., Smillie, L. B., and Reinach, F. C. (1994) *J. Biol. Chem. 269*, 5230−5240.
20. Kobayashi, T., Tao, T., Gergely, J., and Collins, J. H. (1994) *J. Biol. Chem. 269*, 5725−5729.
21. Tripet, B., Van Eyk, J. E., and Hodges, R. S. (1997) *J. Mol. Biol. 271*, 728−750.
22. McKay, R. T., Tripet, B. P., Hodges, R. S., and Sykes, B. D. (1997) *J. Biol. Chem. 272*, 28494−28500.

23. Leszyk, J., Tao, T., Nuwaysir, L. M., and Gergely, J. (1998) *J. Muscle Res. Cell Motil. 19*, 479−490.
24. Leszyk, J., Collins, J. H., Leavis, P. C., and Tao, T. (1987) *Biochemistry 26*, 7042−7047.
25. Kobayashi, T., Tao, T., Grabarek, Z., Gergely, J., and Collins, J. H. (1991) *J. Biol. Chem. 266*, 13746−13751.
26. Greaser, M. L., Yamaguchi, M., Brekke, C., Potter, J. D., and Gergely, J. (1973) *Cold Spring Harbor Symp. Quant. Biol. 37*, 235−244.
27. Greaser, M. L., and Gergely, J. (1971) *J. Biol. Chem. 246*, 4226−4233.
28. Spudich, J. A., and Watt, S. (1971) *J. Biol. Chem. 246*, 4866−4871.
29. Wagner, P. D., and Yount, R. G. (1975) *Biochemistry 14*, 1900−1907.
30. Weeds, A. G., and Taylor, R. S. (1975) *Nature 257*, 54−56.
31. Wang, Z., Sarkar, S., Gergely, J., and Tao, T. (1990) *J. Biol. Chem. 265*, 4953−4957.
32. Luo, Y., Wu, J.-L., Gergely, J., and Tao, T. (1998) *Biophys. J. 74*, 3111−3119.
33. Luo, Y., Wu, J.-L., Gergely, J., and Tao, T. (1997) *Biochemistry 36*, 11027−11035.
34. Leszyk, J., Grabarek, Z., Gergely, J., and Collins, J. H. (1990) *Biochemistry 29*, 299−304.
35. Pearlstone, J. R., Sykes, B. D., and Smillie, L. B. (1997) *Biochemistry 36*, 7601−7606.
36. Vassylyev, D. G., Takeda, S., Wakatsuki, S., Maeda, K., and Maeda, Y. (1998) *Proc. Natl. Acad. Sci. U.S.A. 95*, 4847−4852.
37. Tao, T., Gong, B.-J., and Gergely, J. (1997) *Biophys. J. 72*, A59.
38. Luo, Y., Qian, Y., Wu, J.-L., Gergely, J., and T., T. (1997) *Biophys. J. 72*, A331.

BI9824341